Malaysian Journal of Chemistry, 2025, Vol. 27(3), 427-437
(Special Issue: *International Conference on Sustainable Materials and Technologies, ICSMT 2025*)

Enhancing Compressive Strength of Additively Manufactured Polylactic Acid Composites using Simultaneous Impregnation Extrusion and Carbon Fiber Reinforcement

Sengottaiyan, M.*, Eswaran, S., Amal Quais, R., Rokumar, S. and Rohan, S.
Department of Mechanical Engineering, Nandha Engineering College, Perundurai 638052, Tamil Nadu, India
*Corresponding author (e-mail: sengottaiyan.malaisamy@nandhaengg.org)

Improving the strength and stiffness of additively manufactured components has recently attracted a lot of attention from engineers and scientists. This study found that using an additive manufacturing approach based on simultaneous impregnation extrusion (SIE) increased the compression of polylactic acid (PLA) composites strengthened with carbon fibers (CFs). By employing a side nozzle, this technique coats fibers with molten polymer before depositing them onto a substrate or layers that have already been laid. Without the necessity for pre-impregnated fibers, this approach can be applied to a wide variety of reinforcing phases and matrices, which is its primary advantage. There is a wide variety of fibers and thermoplastics to choose from. We examined tensile lateral strain in compression by placing the fibers perpendicular and parallel to the load direction. Because of this, we were able to determine the effect of fiber orientation. When tested with parallel and perpendicular raster orientations, pristine PLA showed compressive values of 84.6 MPa and 72.3 MPa, respectively. Because the fibers were aligned in a parallel pattern, the composite samples showed separation among the PLA and CF, and they had a compression properties of 41.8±1.3 MPa. But when the fibers were aligned perpendicularly, the compressive strength went up to 94±1.2 MPa. Findings from this study mostly pertain to a method for enhancing composite samples' compressive strength by inserting fibers at an angle. When a compressive force is applied, this design causes transverse strain. Composite samples exhibit improved compressive strength as a result of tensile stress applied to fibers. Tensile stress acting in the opposite direction was applied to several spots, particularly the ends of polished squared cross-sections, where these samples cracked. This study proves that by inserting CFs vertical to the loading track, compression is increased by about 11 % due to the brittle-like fracture and bilinear elastic behavior. Important new information regarding how to make car parts more impact and accident resistant has emerged from these studies.

Keywords: Polylactic acid; compressive strength; extrusion-based 3D printing; additive manufacturing; carbon fibers

Received: February 2025; Accepted: May 2025

The advent of additive manufacturing (AM) has completely altered the product development and assembly processes. New opportunities and threats keep cropping up as AM technologies become more integrated into people's daily lives [1]. This cutting-edge technology has the potential to revolutionize production in the future by making complicated structures that were previously impossible to achieve using conventional methods of manufacture. Some of the main benefits of AM are: The ability to facilitate complex, one-of-a-kind designs that are suited to individual demands is known as customization. The ability to quickly change designs without expensive retooling is an example of flexibility. De-cluttering product designs to speed up development. To cut down on downtime and inventory expenses, efficient spare parts management allows for replacements to be made on demand. Shortening Product Development Cycles and Lead Times. Environmental friendliness and waste reduction are key to sustainability [2]. Fused filament fabrication is one of the most well-known AM processes. It can make lattice structures, which are in great demand because of their strength-to-weight ratio Using FFF to construct anything involves layering molten thermoplastic filament. Due to its low environmental impact, this approach is ideal for the fabrication of cellular structures [3]. For lattice structures, FFF is becoming more common since it is less expensive than alternative technologies like Electron Beam Melting (EBM) and Selective Laser Melting (SLM). A number of process parameters, including nozzle temperature, layer thickness, printing angles, and infill density, need to be precisely managed for FFF to work [4]. The product's mechanical and physical qualities are greatly affected by these elements. Although FFF is typically applied to PLA and ABS, it may also be used with TPU, nylon, and HIPS, which increases the variety of thermoplastics that can be designed with [5]. To attain the targeted level of strength and accuracy, process parameter optimization

†Paper presented at the International Conference on Sustainable Materials and Technologies (ICSMT 2025)

is essential. Surface finish, dimensional correctness, tensile and compressive strength, and other properties may be enhanced by modifying these parameters, according to studies. For instance, by utilizing a genetic algorithm, they were able to optimize the compressive strength of ABS to 17.5 MPa. Additionally, our results from utilizing ANOVA and the Taguchi technique demonstrate that road width and layer thickness have a substantial impact on the surface roughness and size accurateness of ABS components [6]. Along with that, additional materials like PEEK and PETG have demonstrated encouraging results. In FFF applications, PEEK's mechanical properties were better than ABS's, and PETG's compressive strength was greater than ABS's. In order to fully realize FFF's potential, there is an increasing amount of research that focuses on improving process parameters and investigating alternative materials [7]. The influence on the mechanical characteristics of poly lactic acid and ABS lattice pattern by changing the printing speeds, layer thicknesses, and nozzle temperatures. While these investigations did find some optimization potential, they also showed that other parameters need to be investigated more. In terms of build orientations and infill patterns, the results demonstrated that grid patterns were the strongest and most stiff [8]. Reinforcement techniques have also been the subject of research. How mechanical performance is affected by material choice and reinforcement. Nylon composites reinforced with short carbon fibers, for instance, had better tensile and flexural properties than pure nylon, despite the fact that they had lower compressive strength [9]. There has been a lack of research on the effects of mechanical behavior differences on FFF procedures, despite the fact that these variations are prevalent in thermoplastics and very intricate multi-material builds. Enhanced embrittlement and substantial stability benefits were observed in extremely uncommon instances, such as polyamide-6 matrices reinforced with isotropic and concentric carbon fibers. Improving performance requires lowering layer delamination since reinforcing patterns, distribution, and orientation greatly affect compressive and fracture parameters [10]. As a result of ongoing studies, we still have a lot to discover regarding the material characteristics of components made by additive manufacturing. Using propylene fumarate dimethacrylate polyHIPE scaffolds with PLA and PCL outer layers, structural tests were conducted to determine the mechanical properties under compression. It was found that scaffolds made of PLA had a compressive strength (CS) of 4.2 MPa, modulus of 35 MPa and a while scaffold made of PCL had a value of 15 MPa. Specifically, the impact of double extrusion on the compressive mechanical characteristics of polymeric nanocomposites based on clay was examined [11]. Twin extrusion technology improved Nano clay mixing, which in turn raised the printed samples' tensile strength by 14.5 %, tensile modulus by 21%, and compressive strength by 24 %. Under compressive circumstances with strain rates between 1.4- and 180-mm min^{-1}, PMMA's compressive strength improved by 40% and TPU's compressive modulus by 29%. In terms of material sensitivity to strain rates, PC was the most sensitive. 3D printed polyimide aerogels with improved compressive mechanical characteristics using an extrusion-based freeze casting process [12]. The modulus was increased to 63.5 MPa and the maximum compressive strength to 6.35 MPa for the printed polyimide aerogel samples. Researchers looked examined PETG composites with 2, 5, or 10 % silk fiber reinforcement by weight to show how they fared mechanically. According to their findings, production with 15 % silk fibers was difficult, but the composite with 2.5 % silk fibers had a 65 % higher compressive modulus than plain PETG [13]. Composites made of PLA and Ti6Al4V (Ti64) and their mechanical characteristics. Their research showed that incorporating Ti64 into PLA raised its carbon transition temperature but somewhat lowered its melting point, crystallization point, and thermal stability rasters. The composite's modulus was 1.9 GPa and compressive strength was 49.9 MPa, both of which were enhanced by adding 3 % to 6 % by weight of Ti64. We will conclude by investigating how PC-ABS blend creep displacement is affected by printing parameters. We discovered that the parameters that produced the least amount of creep displacement were as follows: 0.2540 mm layer height, 0° raster angle, 20° print direction, eight shells, and 0.4572 mm extrusion width [14]. Analyzing the mechanical and structural properties of bi-matrix composites augmented with fibers and different cavities by 3D printing. Carbon fibers, PLA and PA filaments, continuous carbon fibers, and epoxy-impregnated basalt were all used to make the examples. According to their findings, the mechanical properties and failure mechanism are mainly affected by continuous carbon fibers that have been pre-impregnated with epoxy resin after printing. Results showed that pullout and fiber breakage were the most common causes of failure in this study. Various fiber-reinforced 3D-printed polymer matrix composites' fracture toughness [15]. Two matrices with different melting points were considered: PLA and PEEK. Mechanical characteristics and fracture performance of printed materials are negatively affected by factors such printing speed, layer thickness, voids, porosity, and a circular nozzle shape. Alternatively, things like printing in a vacuum, fiber length, annealing, printing in different directions, printing with the right surface treatment on the fibers, and printing at a specific temperature all work to the advantage. The simultaneous fiber-polymer impregnation approach was used to successfully install continuous carbon fibers on curved surfaces by delivering a 3D G-code. Micro-carbon fiber, copper, and bronze reinforced composites made by 3D printing and their mechanical and thermal characteristics. The Filling percentage of 60 %, and layer thickness of 0.1 mm, Nozzle temperature of 230°C, were found to be the best parameters for producing maximum tensile strength. While adding metal reinforcing particles increased elongation, they decreased strength. In addition, when it comes to heat resistance, nothing beats PLA-Cu composites [16]. The compressive

characteristics and printing parameters of hybrid composites composed of neat PLA and PLA strengthened with almond shell are examined in this work. A highest compression property of 36.78 MPa was achieved by printing with 20 mm/s, 0.1 mm layer height, and 200°C. CF composites made by additive manufacturing with PEEK as the foundation material: specifications [17]. The bending strength was 506 MPa, the impact strength was 54 MPa, the interlaminar shear strength was 44 MPa, and the highest tensile strength was 180 kJ/m^2. Examination of the impact of printing temperature on the mechanical characteristics of ABS filaments. Between 220 and 270°C, a 10°C rise, they discovered that the printed materials' mass and tensile strength decreased roughly linearly with rising temperature. A tensile characteristic of 24.6 MPa was measured at 220°C, with a value of 14.4 MPa obtained at 270°C, being the lowest. Printed components' energy absorption capabilities and auxetic structures' mechanical characteristics as a result of fed-forward and multi-jet production. The purpose of this contribution is to examine the elastic, failure, and fracture properties of a composite strengthened with CFs and to draw conclusions on the feasibility of using this reinforcement with polylactic acid (PLA) based on a comprehensive literature search. The behavior of cracks in 3D-printed PLA composites reinforced with continuous carbon fiber is an initial focus of this research [18]. This research primarily aims to examine the impact of fibers on the compressive mechanical characteristics of 3D printed composite materials. We have examined both parallel and perpendicular configurations to take into consideration the impact of the deposition approach on the direction of the compression load. Scanning electron microscopy (SEM) analysis of PLA fracture surfaces, both filled and unfilled, has also demonstrated that composite mechanical compressive properties can be enhanced by redistributing compressive loads to tensile deformation, which occurs when fiber orientation is changed. As a result, the material's general behavior changes and its compressive strength improves by around 10%.

EXPERIMENTAL METHODOLOGY

The matrix material utilized in this investigation is polylactic acid (PLA) filament. The datasheet from the manufacturer states that the filament's glass transition temperature is 80°C. The reinforcement was made of carbon continuous fiber yarn. It had a 0.12 g/m and a 0.3 mm diameter (7 µm fiber diameter, Tex 0.8 g/m). Datasheet specifications for carbon fiber yarn include 1.95 g/cm² density, 3000 MPa nominal tensile strength, and 600 GPa tensile modulus. In order to confirm the mechanical parameters, tensile tests were performed in accordance with ASTM D2256, which included a tensile strength of 940 MPa, a strain of 0.0172, and a modulus of 68.2 GPa. The materials were sourced from Kovai cheenu enterprises, Coimbatore, India. Fig. 1(a) and Fig. 1(b) displays the tensile stress vs strain curve that was produced from tensile testing for continuous carbon fibers (mean from 10^{-3} specimen) and PLA (averaged from 5 samples).

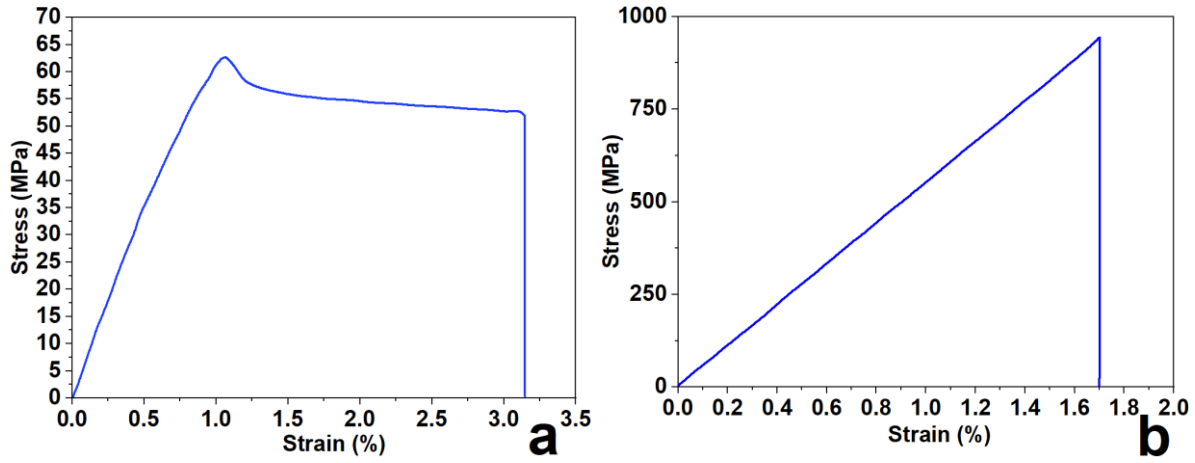

Figure 1. Evaluation of Tensile properties of stress vs strain curve for (a) Poly lactic acid and (b) CF.

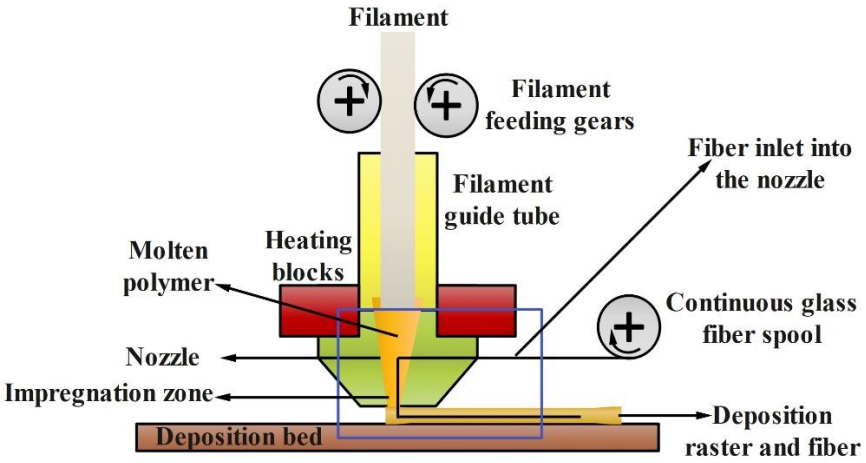

Figure 2. Illustrations of the SIE process and a detailed description of the employed FFF technique.

Figure 2 shows the substrate being covered with carbon fibers that have been infused with melted PLA polymers using the utilized simultaneous impregnation extrusion (SIE) process. The Quantum 2020 3D printer, which aimed for a 30 % fiber volume percentage was used for manufacturing. The bed size of the printer was 200×200×200 mm. The percentage of fiber volume was determined experimentally by burning samples following mechanical testing and then weighing the leftover fibers after washing and drying. The volume percentage was then calculated from the weight percentage of fibers in accordance with ASTM D3171. The PLA with CF composite specimen deviated slightly from the theoretical objective by around 2 %, with an experimentally estimated fiber proportion percentage of 31.5 %. To keep printing consistent and avoid overflow, the PLA nourishing speed has to be changed, since fibers decrease the amount of extruded polymer that is available [19]. Following calibration, it was found that 10 mm/s was the ideal printing speed for the PLA-CF composite, guaranteeing uniform deposition free from excess or lack of material. For each test, five samples were printed to assess mechanical qualities, and the findings were given as an average. Fibers and polymer materials are impregnated more effectively when the nozzle temperature rises because the polymer material's viscosity drops. But if the nozzle becomes too hot, the polymer will degrade, and the surface quality will suffer in that direction as well. Based on previous studies that employed the same dataset. The researchers in this investigation found that 230°C was the best for both material integrity and fiber impregnation. The primary layers' substrate temperature is particularly important for appropriate inter raster and interfacial adhesion. Keeping the substrate temperature below the polymer's carbon transition temperature 85°C for the poly lactic acid used here is critical to avert substratum salving and inadvertent divan separation. Because of this, 60°C was settled upon as the bed temperature. The layers' heights in relation to the fibers' diameters also need careful consideration [20]. Layer heights that are lower than fiber diameters increase the likelihood of fiber breakage during manufacture. However, the build direction surface will be more uneven and the printed sample will have holes in it if the nozzle height is set too high. The researchers in this study took these considerations into account by adjusting the layer height to 0.23 mm (the diameter of the fiber) and the extruded thickness to 0.60 mm (the percentage of fiber volume), for a total of 30 %. By plugging the fiber diameter (df), extrusion width (w), and layer height (h) into equation (1), we can determine the fiber volume percentage as a percentage of the matrix volume.

$$V_f = \left(\pi d_f^2/4 \cdot w \cdot h\right) \times 100 \quad (1)$$

In order to keep the extrusion process going while the fibers and polymer matrix are mixed, it is necessary to use less polymer. To fix it, in the G-code, the need to multiply a coefficient called the extrusion multiplier by the filament feed parameter, which is denoted as 'V_f'. In order to determine the extruded multiplier (F), one uses formulation (2).

$$F = 1 - V_f \quad (2)$$

Both the unfilled PLA and the composite material are listed as raw materials in table 1 for the purpose of comparing their compressive properties. Compressive qualities were assessed using specimens made according to ASTM D695 standards; these specimens had a 12.8 mm square cross-section and a 26.5 mm height, as illustrated in Figure 3.

Table 1. Printing settings for PLA-CF composites and unfilled PLA filaments.

Factors	Units	Range
Height of Extrusion layer (raster)	[mm]	0.23
Nozzle diameter	[mm]	0.6
Speed of filament feeding	[mm s^{-1}]	45/10
Nozzle temperature	[°C]	225
Extrusion width (raster)	[mm]	0.59
Deposition bed temperature	[°C]	65
Neat PLA vs PLA with CF composite Extruded multiplier		0.8

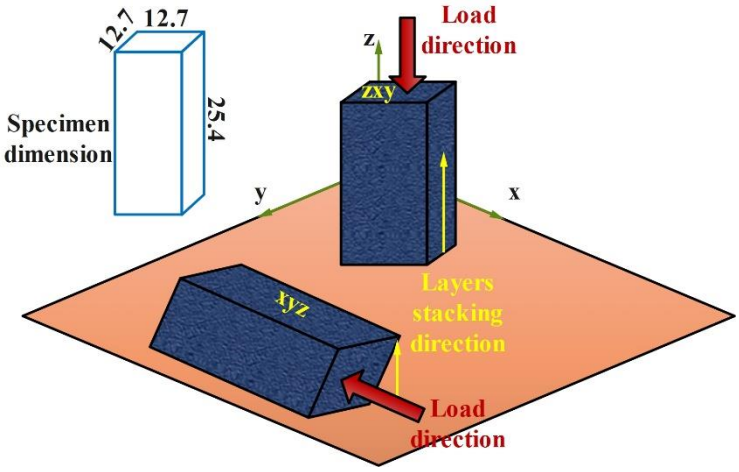

Figure 3. The 'H' and 'V' orientations dictate the stacking orientation for the PLA-CF sample.

Two batches of specimens were manufactured in order to evaluate the efficacy of the CF reinforcement. With the first set of coordinates, "XYZ," also known as the "H" orientation, the specimen's height is tracked along a rising plane. This design results in some fibers experiencing compressive strains and others experiencing tensile strains when a load is applied along the x-axis of the load. In the "V" configuration, often called specimens 'ZXY,' compression test specimens showed fibers lined up in a concentrical arrangement, axes by axes, perpendicular to the z-axes. Neat PLA samples with the similar raster orientation were also included in the standards stated above, in addition to the composite PLA-CF specimens. The blank PLA and PLA-CF composite specimens were subjected to compression at a rate of 5 mm/min. Following testing, a ZEISS SEM was used to analyze the failure surfaces. This allowed researchers to gain a better understanding of the matrix and fibers' interactions and responsibilities when under strain.

RESULTS AND DISCUSSIONS

An outcome of compressive tests performed on pure poly lactic acid and composites comprising CF components are presented in this section. Afterwards, a scanning electron microscopy (SEM) analysis was conducted on the failure surfaces. Following this, we will note any pertinent details and derive any inferences from the results. The printed samples' energy absorption characteristics are mentioned lastly.

Results on Compression Properties

The uniaxial compressive strength magnifies tensile and compressive deformations by placing a vertical force on top of the material. A small deformation zone called the deceased substantial region forms around the point of contact and the specimen's sides undergo barreling as a result of the frictional interface among the top and bottom jaw as illustrated in Figure 4.

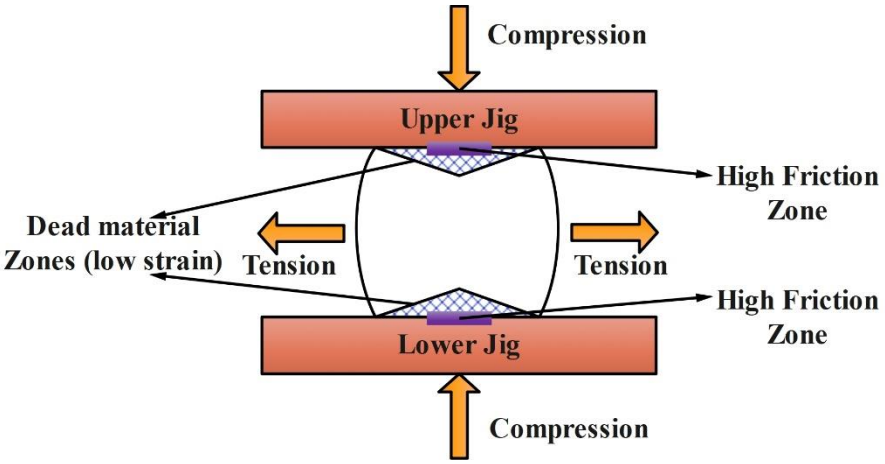

Figure 4. The distortion characteristics of the uniaxial compressive test.

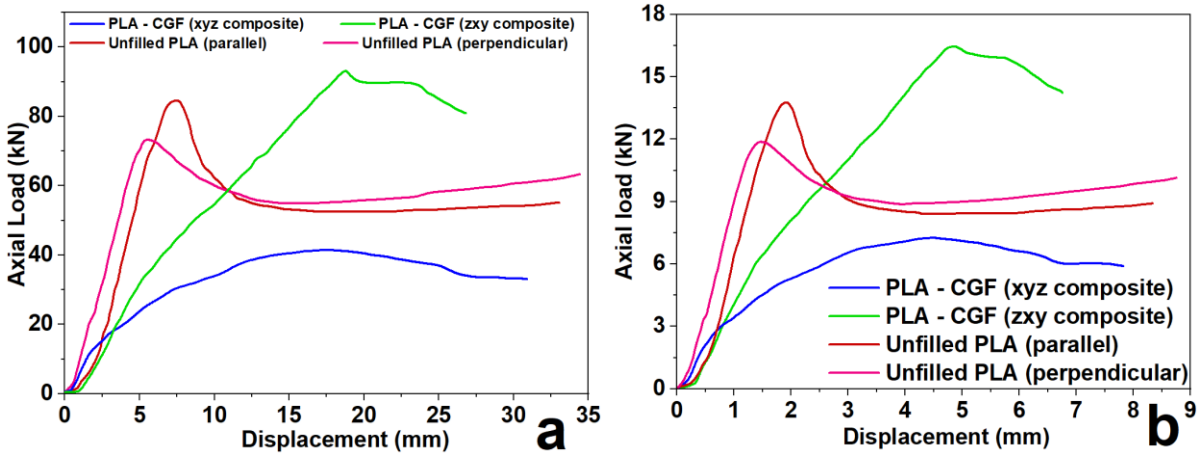

Figure 5. (a) Compressive stress vs strain curve for Neat PLA and PLA with CF for H and V orientations **(b)** Compressive axial force against displacement curve for Neat PLA and PLA with CF for H and V orientations.

As a result, the specimen experiences simultaneous compressive and tensile deformations throughout the test. Composite materials like PLA-CF exhibit deformation behavior that is drastically different from that of its constituent parts because of the unique reactions and interactions of these parts. Fig. 5(a) shows the mean stress-strain curves from 5 trials test for the without PLA and PLA with CF composite sample that were subjected to compression tests. Figure 5(b) depicts the compressive axial force against displacement curve for Neat PLA and PLA with CF for H and V orientations respectively.

Raster alignment with the compressive load track increases the strength of without PLA specimens by about 17 %. The raster, which serve as separate units that bear the weight of the compression, are partially oriented, which is responsible for this enhancement. In contrast, raster behavior is characterized as isotropic when it is deposited plane by plane in a direction perpendicular to compression [21]. When subjected to buckling, even perfectly aligned PLA specimens will fail. Figure 6 displays scanning electron micrographs of clean PLA sample cross-sections.

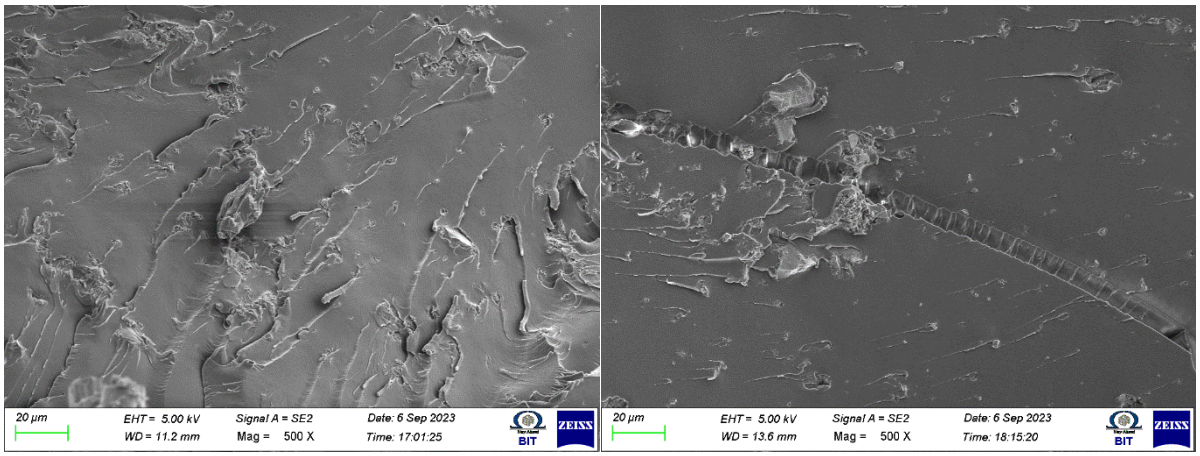

Figure. 6. Cross-sectional SEM images of pure polymer (a) V orientation and (b) H orientation.

The samples that made it through the compression tests were then placed in liquid nitrogen to freeze until they could be broken for analysis. The lack of visible seams in the cross-sectional photos is evidence that the printing settings were optimal, since the rasters and layers were all properly connected [22]. Both of the unfilled PLA specimens have the following compressive strengths and moduli:

- Perpendicular rasters: 73.4 ± 0.8 MPa and 1.8 ± 0.06 GPa.
- Parallel rasters: 85.7 ± 1.2 MPa and 1.9 ± 0.05 GPa.

The correlation between stress, percentage strain, and compressive strength for PLA-CF compression specimens is significantly affected by the deposition process and how it interacts with the applying compression load. Within the dead material zone, H specimens (Fig. 3) get compressed in the polymer matrix and tensed in the fibers. The specimen is compressed along the x-axes and the PLA is under stress in the y axes and z axes, as shown in Figure 7(a). This compression is most noticeable around the specimen's center, where barreling occurs. Therefore, the H PLA-CF specimens shouldn't fail at the dead material zone, but rather anywhere in the center. The failure occurs when the fibers undergo compressive deformation at the same time that the PLA matrix undergoes tensile deformation, which causes the fiber-matrix contact to buckle and debond [23]. Here, the exact percentage of compressive strength gains over empty PLA varies from 10.5 % to 29.3 %, depending on the orientation of the raster with regard to the compressive force. Not only that, unlike unfilled PLA specimens, which display bilinear behavior in the stress-strain relationship, filled PLA specimens soften after a single peak stress [24]. Since the pure matrix and composite samples exhibit clearly different elastic and elastic-plastic behaviors, the bilinear response is typical of designs involving multiple materials [25].

The rasters and continuous carbon fibers in the V specimens are perpendicular to the compressive load. Reinforcement efficiency is decreased in this direction when related to the H orientation. As displayed in Fig. 5(a), CFs smooth out the stress-strain connection. This causes the stress to rise steadily until it reaches its maximum, after which it slightly decreases immediately before failure [26, 27]. In this arrangement, the z-axis is compressed, while the x and y axes represent stress vectors in the matrix and fibers, respectively (Figure 7(b)). Debonding is more prone to happen at the square corners of tensioned fibers that are resting in the xy planes, as illustrated in Figure 7(c), when the stress direction changes from x to y [28, 29]. Due to the fibers' alignment perpendicular to the compressive load, rather than serving as reinforcements, they behave as inclusions in the PLA-CF composite, leading to a matrix-dominated fracture [30, 31]. There is a 2.3-fold variation in strength between the H and V forms, which is typical of composite materials. This discovery highlights the practicality of CFs in enhancing PLA matrix properties. Finally, the modulus and compressive strength are, respectively,

- PLA-CF (V): 94.6 ± 1.3 MPa and 0.87 ± 0.03 GPa.
- PLA-CF (H): 41.8 ± 1.3 MPa and 0.89 ± 0.03 GPa.

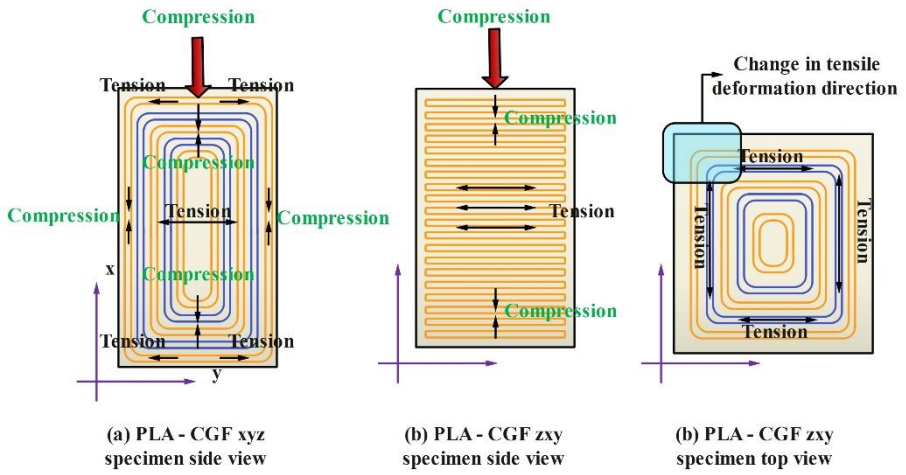

Figure 7. The PLA-CF composite demonstrated compressive and tensile behavior in the following specimens: The H specimen (forward-facing view), the V specimen (forward-facing view), and the V specimen (topmost view).

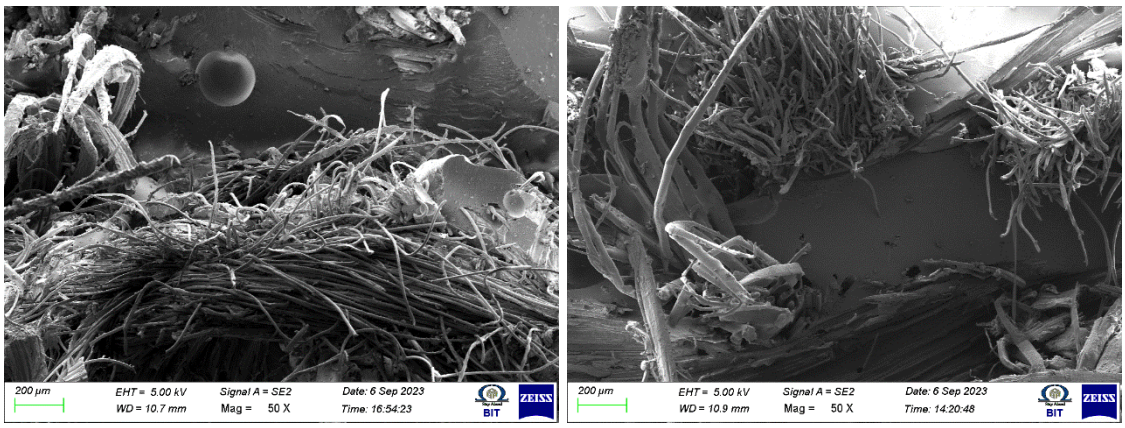

Figure 8. SEM analysis of PLA-CF samples on (a) H and (b) V fiber orientation.

To validate the theories about deformation, debonding, and buckling, and to delve deeper into the behavior of the two PLA-CF composite configurations that were evaluated, scanning electron microscopy (SEM) investigations were performed. Figure 8(a) shows that when the PLA matrix is pulled taut, the H composite separates in the middle of the specimen. The PLA matrix and CFs debond because to this tensile stress. Also, as predicted, the carbon fibers buckle under the stress of the PLA matrix's tensile deformation, debonding from the matrix and producing noticeable fracture surface tracks [31, 32].

Alternatively, the V composite shows that the CFs had a completely insignificant function in supporting the compression load throughout the tests. Figure 8(b) shows that there is very little fibrillation and clean matrix separation on the fracture surface. In addition, fibers separate from the matrix in bundles, a phenomenon known as fiber pull-out, which mirrors the pattern of fiber deposition during FFF.

Characteristics of Energy Absorption

Figure 5(b) shows the force vs displacement curve of the specimen, which corresponds to the stress-strain diagram in terms of behavior. In Table 2, the crushing parameters of the samples are summarized using the data from Figure 5(b). Among these numbers are the following: total absorbed energy, specific absorbed energy, mean crush force, and initial peak force.

Table 2. The compression specimens of neat PLA and PLA-CF exhibit crushing behaviour.

Crushing behaviour	Neat PLA (H-orientation)	Neat PLA (V-orientation)	PLA with CF (H-orientation)	PLA with CF (V-orientation)
Starting Peak Force (kN)	14.66	12.70	7.92	17.47
Average Crushing Force (kN)	9.35	9.91	6.45	11.70
Overall Absorbed Energy (J)	67.79	75.59	41.72	69.75
Specific Absorbed Energy (J/g)	14.05	15.58	7.05	11.22
Crushing Force Efficacy	0.72	0.87	0.90	0.76

The composite material's starting maximum force and average crushing force range are at their maximum when the grain orientation is vertical to the load's application path. This is because the sample's improved compressive strength is affected by the transverse strain [33, 34]. Unfilled PLA samples had higher specific and total absorbed energies compared to the composite samples, which are the polar opposite. While the composite samples do demonstrate an improvement in compressive strength, it seems that there is space for improvement in their energy absorption capabilities. It follows that modifying the geometrical of the composite specimen can improve crashworthiness and help understand the impact of geometry on crushing parameters [35, 36].

CONCLUSIONS

This work was conducted to examine the compression property and crack behavior of CF-strengthened poly lactic acid composites that were manufactured using a unique SIE process. By positioning CFs perpendicular to the direction of load application, it was found that the CS of empty PLA may be enhanced between 11 % and 30 %. But CFs lose most of their reinforcing function and the matrix's strength and toughness when they're laid out perpendicular to the direction of the load. Bilinear quasi-brittle performance in the horizontal position and nearly no hardening and result in in the vertical position were among the remarkable mechanical properties observed in the PLA-CF composite in comparison to neat PLA. These results demonstrate that the mechanical behaviour of the composites is highly dependent on the orientation of the CF. This kind of research also demonstrates the potential utility of CFs and the fact that composites can be made using the SIE technique, even with acute (90°) twists. The experimental results demonstrate that the mechanical characteristics of 3D printing composites are significantly impacted by the orientation of the continuous filament. When compared to the untreated PLA samples, the PLA-CF V composite showed a 30 % increase in initial peak force (16.46 kN) and a 24 % increase in mean crush force (10.69 kN). These findings point to the possibility of using PLA-CF composites to make energy-absorbing parts more crash-proof. Research in the future should look into using high-modulus reinforcements, including continuous carbon fibers, and how the fraction of fiber volume affects compressive mechanical qualities. This area of study has the potential to improve energy-absorbing components' crashworthiness in a variety of applications.

REFERENCES

1. Billings, C., Siddique, R., Sherwood, B., Hall, J. and Liu, Y. (2023) Additive Manufacturing and Characterization of Sustainable Wood Fiber-Reinforced Green Composites. *Journal of Composites Science*, **7,** 489.

2. Orisekeh, D. K., Corti, G. and Jahan, M. P. (2025) Enhancing thermo-mechanical properties of additively manufactured PLA using eggshell microparticle fillers. *Journal of Manufacturing Processes*, **133**, 782–797.

3. Manickam, T., Iyyadurai, J., Jaganathan, M., Babuchellam, A., Mayakrishnan, M. and Arockiasamy, F.S. (2023) Effect of stacking sequence on mechanical, water absorption, and biodegradable properties of novel hybrid composites for structural applications. *International Polymer Processing,* **38,** 88–96.

4. Jeyaprakasam, S., Gnanasekaran, M., Magibalan, S., Singh, R.P., Mohanavel, V., Kannan, S., Giri, J., Ali, M.S. and Barmavatu, P. (2024) Tribological, mechanical and microstructure characteristics of hybrid aluminium matrix composite containing

titanium carbide (TiC) and graphite particles. *Journal of Materials Research and Technology,* **33,** 5482–5489.

4. Siddiqui, V. U., Yusuf, J., Sapuan, S. M., Hasan, M. Z., Mudah Bistari, M. M. and Mohammadsalih, Z. G. (2024) Mechanical properties and flammability analysis of wood fiber filled polylactic acid (PLA) composites using additive manufacturing. *Journal of Natural Fibers*, **21**, 2409868.

5. Xing, D., Wang, H., Tao, Y., Zhang, J., Li, P. and Koubaa, A. (2024) 3D-printing continuous plant fiber/polylactic acid composites with lightweight and high strength. *Polymer Composites*.

6. Mishra, V. and Veeman, D. (2025) Artificial neural network-based predictive models for analyzing the flexural and compressive strength of PLA/ carbon parts fabricated via material extrusion-based 3D printing. *Journal of Thermoplastic Composite Materials*.

7. Vasumathi, M., Karupaiah, V. and Narayanan, V. (2024) Effect of process parameters on mechanical and tribological characteristics of FDM printed glass fiber reinforced PLA composites. *Rapid Prototyping Journal*, **30**, 1859–1875.

8. Farrokhabadi, A., Lu, H., Yang, X., Rauf, A., Talemi, R., Behravesh, A. H., Hedayati, S. K. and Chronopoulos, D. (2024) Energy absorption assessment of recovered shapes in 3D-printed star hourglass honeycombs: Experimental and numerical approaches. *Composite Structures*, **347**, 118444.

9. Vieweger, D., Diel, S., Schweiger, H. G. and Tetzlaff, U. (2024) Mechanical Properties of Raw Filaments and Printed Specimens: Effects of Fiber Reinforcements and Process Parameters. *Polymers*, **16**, 1576.

10. Dani, M.S., Saravanan, N., Girisha, L., Uday, K.K., Ramalingam, R., Nanthakumar, S., Girimurugan, R., Anbarasu, M. and Mathanbabu, M. (2024) Optimizing the Properties of AA 5052 Alloys through Silicon Carbide and Groundnut Shell Ash Reinforcements. *International Journal of Vehicle Structures & Systems,* **16,** 630–635.

11. Farrokhabadi, A., Lu, H., Yang, X., Rauf, A., Talemi, R., Behravesh, A. H., Hedayati, S. K. and Chronopoulos, D. (2024) Energy absorption assessment of recovered shapes in 3D-printed star hourglass honeycombs: Experimental and numerical approaches. *Composite Structures,* **347,** 118444.

12. Liang, L., Yan, L., Cao, M., Ji, Z., Cheng, L., Huang, R. and Zheng, L. (2023) Microwave absorption and compression performance design of continuous carbon fiber reinforced 3D printing pyramidal array sandwich structure. *Composites Communications*, **44**, 101773.

13. Nekin Joshua, R. and Aravind Raj, S. (2024) Comparison of quasi-static compression performance of FDM 3D printed truss supported double arrowhead structure with a circular node. *Mechanics of Advanced Materials and Structures*, **31**, 12774–12787.

14. Calles, A. F., Carou, D. and Ferreira, R. L. (2022) Experimental investigation on the effect of carbon fiber reinforcements in the mechanical resistance of 3D printed specimens. *Applied Composite Materials*, **29**, 1–16.

15. Marinopoulos, T., Li, S. and Silberschmidt, V. V. (2023) Structural integrity of 3D-printed prosthetic sockets: Experimental study for paediatric applications. *Journal of Materials Research and Technology*, **24**, 2734–2742.

16. Khawale, V. R., Kumar, R., Satishkumar, P., Haldar, B., Deepa, B., Saminathan, R., Veeramanikandan, P., Packirisamy, A. S. B. and Selvaraju, M. (2024) Study on Electrochemical Stability and Charge Transfer Efficiency for the Development of High-Performance Supercapacitors Using Iron Oxide (Fe_2O_3) Nanorods. Journal of New Materials for Electrochemical Systems, 27, 163–171.

17. Ma, Q., Rejab, M. R. M., Kumar, A. P., Fu, H., Kumar, N. M. and Tang, J. (2021) Effect of infill pattern, density and material type of 3D printed cubic structure under quasi-static loading. *Proceedings of the Institution of Mechanical Engineers, Part C: Journal of Mechanical Engineering Science*, **235**, 4254–4272.

18. Irfan, M. S., Patel, S., Umer, R., Ali, M. A. and Dong, Y. (2022) Thermal and morphological analysis of various 3D printed composite honeycomb cores. Composite Structures, 290, 115517.

19. Zarna, C., Chinga-Carrasco, G. and Echtermeyer, A. T. (2023) Biocomposite panels with unidirectional core stiffeners− 3-point bending properties and considerations on 3D printing and extrusion as a manufacturing method. *Composite Structures*, **313**, 116930.

20. Sugumar, S., Dhamodaran, G., Seetharaman, P. and Sivakumar, R. (2024) Study of Hardness and Compression Strength of Carbon Fibre Reinforced Poly-Lactic Acid Composites Fabricated by Fused Deposition Modelling. *SAE Technical Papers*.

21. Saleh, M., Anwar, S., Al-Ahmari, A. M. and AlFaify, A. Y. (2023) Prediction of mechanical

properties for carbon fiber/PLA composite lattice structures using mathematical and ANFIS models. *Polymers*, **15**, 1720.

22. Thakur, V., Kumar, R., Kumar, R., Singh, R. and Kumar, V. (2024) Hybrid additive manufacturing of highly sustainable Polylactic acid-Carbon Fiber-Polylactic acid sandwiched composite structures: Optimization and machine learning. *Journal of Thermoplastic Composite Materials*, **37,** 466–492.

23. Yang, L., Zhou, L., Lin, Y., Hu, Y., Yan, C. and Shi, Y. (2024) Failure mode analysis and prediction model of additively manufactured continuous carbon fiber-reinforced polylactic acid. *Polymer Composites*, **45**, 7205–7221.

24. Shah, A. K. and Jain, A. (2024) Microstructure and mechanical properties of filament and fused deposition modelling printed polylactic-acid and carbon-fiber reinforced polylactic-acid. *Journal of Reinforced Plastics and Composites*, **43,** 516–531.

25. Jain, A., Mishra, A., Dubey, A. K., Kumar, A., Sahai, A. and Sharma, R. S. (2023) Mechanical characteristics and failure morphology of FFF-printed poly lactic acid composites reinforced with carbon fibre, graphene and MWCNTs. *Journal of Thermoplastic Composite Materials*, **36**, 3618–3643.

26. Abas, M., Habib, T., Khan, I. and Noor, S. (2025) Definitive screening design for mechanical properties enhancement in extrusion-based additive manufacturing of carbon fiber-reinforced PLA composite. *Progress in Additive Manufacturing,* **10**, 139–157.

27. Chen, Y., Wei, X., Mao, J., Zhao, M. and Liu, G. (2024) Experimental analysis of 3D printed continuous carbon/glass hybrid fiber reinforced PLA composites: Revealing synergistic mechanical properties and failure mechanisms. *Polymer Composites,* **45**, 10888–10897.

28. Zou, L., Zuo, H., Dou, T., Wang, H., Sun, Y., Liu, L., Ming Yao, Fangtao Ruan and Zhenzhen Xu (2024) 3D printing of carbon fiber powder/ polylactic acid with enhanced electromagnetic interference shielding. *Diamond and Related Materials*, **141**, 110583.

29. Saleh, M., Anwar, S., AlFaify, A. Y., Al-Ahmari, A. M. and Abd Elgawad, A. E. E. (2024) Development of PLA/recycled-desized carbon fiber composites for 3D printing: Thermal, mechanical, and morphological analyses. *Journal of Materials Research and Technology,* **29**, 2768–2780.

30. Adil, S. and Lazoglu, I. (2023) A review on additive manufacturing of carbon fiber-reinforced polymers: Current methods, materials, mechanical properties, applications and challenges. *Journal of Applied Polymer Science*, **140**, 53476.

31. Thirugnanasamabandam, A., Subramaniyan, M., Prabhu, B. and Ramachandran, K. (2024) Development and comprehensive investigation on PLA/carbon fiber reinforced PLA based structurally alternate layered polymer composites. *Journal of Industrial and Engineering Chemistry*, **136**, 248–257.

32. Khalili, A., Kami, A. and Abedini, V. (2023) Tensile and flexural properties of 3D-printed polylactic acid/continuous carbon fiber composite. *Mechanics of Advanced Composite Structures*, **10**, 407–418.

33. Kargar, E. and Ghasemi-Ghalebahman, A. (2023) Experimental investigation on fatigue life and tensile strength of carbon fiber-reinforced PLA composites based on fused deposition modeling. *Scientific Reports*, **13**, 18194.

34. Cao, A., Wan, D., Gao, C. and Elverum, C. W. (2024) A novel method of fabricating designable polylactic acid (PLA)/thermoplastic polyurethane (TPU) composite filaments and structures by material extrusion additive manufacturing. *Journal of Manufacturing Processes*, **118**, 432–447.

35. Arul, M., Subramaniyan, C., Sakthivelmurugan, E. and Sureshkumar, M. (2024) Optimising mechanical properties of epoxy matrix hybrid composites through SiC filler integration and fiber reinforcement: the Taguchi approach. *Cellulose Chemistry and Technology*, **58**, 591–602.